IOP Publishing Superconductor Science and Technology
Supercond. Sci. Technol. 31 (2018) 015022 (8pp) https://doi.org/10.1088/1361-6668/aa9a6d

High utilization ratio of metal organic sources for MOCVD-derived GdYBCO films based on a narrow channel reaction chamber

Ruipeng Zhao[1], Qing Liu[1], Yudong Xia[2], Hao Tang[1], Yuming Lu[3], Chuanbing Cai[3], Bowan Tao[1] and Yanrong Li[1]

[1] State Key Lab of Electronic Thin Films and Integrated Devices, University of Electronic Science and Technology of China, Chengdu 610054, People's Republic of China
[2] School of Physical Science and Technology, Southwest Jiaotong University, Chengdu 610031, People's Republic of China
[3] School of Physics, Shanghai University, Shanghai 200444, People's Republic of China

E-mail: taobw@uestc.edu.cn

Received 11 September 2017, revised 9 November 2017
Accepted for publication 14 November 2017
Published 13 December 2017

Abstract

A narrow channel reaction chamber is designed in our home-made MOCVD system and applied to deposit GdYBCO films on the template of $LaMnO_3$/epitaxial MgO/IBAD-MgO/solution deposition planarization-Y_2O_3-buffered Hastelloy tapes. In the reaction chamber, metal organic sources are transferred from the inlet to the outlet along the direction of the tape movement. Thus, compared to the vertical injection way of metal organic sources, the residence time of metal organic sources on the surface of substrates would be extended through adopting the novel reaction chamber. Therefore, the utilization of metal organic sources, which is calculated according to the measured results of experiments, can reach 31%. Additionally, the utilization ratio of metal organic sources based on the novel reaction chamber is basically two times as much as that of the commonly used vertical injection slit shower. What is more, through adjusting the process, the critical current density of 300 nm thick GdYBCO film prepared the reel-to-reel way has reached 3.2 MA cm^{-2} (77 K, 0 T).

Keywords: narrow channel reaction chamber, MOCVD, GdYBCO, utilization ratio, critical current density

(Some figures may appear in colour only in the online journal)

1. Introduction

Second-generation $REBa_2Cu_3O_{7-\delta}$ ((REBCO), RE = rare earth) high temperature superconducting (HTS) tapes, also called coated conductors (CCs), have been studied by many researchers of the world because of its excellent property of high current capacity [1–3]. Moreover, they have widespread application prospects in superconducting transmission cables, superconducting motors, superconducting generators, superconducting current limiters, superconducting magnetic energy storage and so on [4–11]. Nowadays, tapes with length of kilometers and critical current of hundreds of amperes have been prepared all over the world [12–16]. However, the excessively high preparation cost limits the application of second-generation REBCO tapes [17–19]. In addition, most of the cost comes from the preparations of the superconducting layer.

Up to now, the main technical routes for the preparation of REBCO superconducting layer have been metal organic deposition [20, 21], pulsed laser deposition [22, 23], reactive co-evaporation [24, 25] and metal organic chemical vapor deposition (MOCVD) [26–29]. Different process

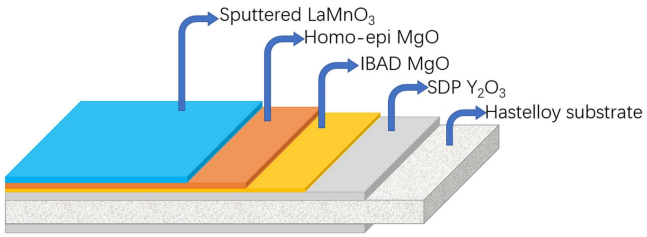

Figure 1. The schematic diagram of the layer stack of buffer layers on the Hastelloy tape.

methods are selected to deposit REBCO films because of their respective characteristics. Hence, MOCVD is adopted by us for the deposition of GdYBCO films because of the advantages of good scalability, high production efficiency, low vacuum requirement and good composition controllability. However, for the MOCVD process method, the commercialization of REBCO tapes is restricted by its high production cost. And the cost of metal organic sources approximately accounts for 50% of the CCs production cost. Therefore, increasing the utilization ratio of metal organic sources is a very effective way to reduce the cost of REBCO tapes. Selvamanickam V *et al* reported the plasma assisted metal organic chemical vapor deposition process being applied to improve the deposition rate and the utilization ratio of metal organic sources [30]. However, the utilization ratio of metal organic sources is basically less than 20% through using the improved MOCVD for the preparation of REBCO films.

In this paper, a narrow channel reaction chamber for the deposition of GdYBCO films is proposed and used in our home-made MOCVD system. To be more specific, in the narrow channel reaction chamber, metal organic sources are transferred from inlet to outlet along the direction of the tape movement. Thus, the residence time of metal organic sources on the surface of substrates would be extended. Therefore, the designed and applied reaction chamber can not only perform the reel-to-reel deposition for double-sided GdYBCO tapes, but also increase the utilization also of metal organic sources, which is believed to be a promising design to improve the cost and performance of second-generation REBCO HTS tapes.

2. Experiment

In our experiments, the substrate used for reel-to-reel metal organic chemical vapor deposition of GdYBCO film was a stack of sputtered-$LaMnO_3$/homo-epitaxial MgO/IBAD-MgO/ solution deposition planarization-Y_2O_3/Hastelloy tapes [31–35], as is shown in figure 1. Heating current (I_h) was conducted from the two edges of the template tape into the Hastelloy metal tape [36, 37]. Then, heat was generated by the joule effect due to its own resistance of the Hastelloy tape. Additionally, the temperature of tapes can be adjusted by the magnitude of conducted I_h. Figure 2 shows the schematic diagram of the GdYBCO film preparation based on the self-heating technique and the narrow channel reaction chamber. As is shown in figure 2(b), the 1 mm × 11 mm slits are formed at both ends of the narrow channel reaction chamber through the use of ceramic plugs and the slit near the inlet is pumped into argon to form a high pressure zone. Thus, the slit and the high pressure zone are designed to prevent the reverse flow of metal organic sources. The tetrahydrofuran solution of Gd(tmhd)$_3$, Y(tmhd)$_3$, Ba(tmhd)$_2$·(1,10-phenanthroline)$_2$ and Cu(tmhd)$_2$ (tmhd: 2,2,6,6,-tetramethyl-3,5-heptanedionate) were evaporated to form vapor in the evaporator. Then the vapor was mixed with the argon, oxygen and nitrous oxide in the gas-flow-ratio of 2.44:1.06:1 and was transferred into the reaction chamber from the inlet for deposition of GdYBCO film on the surface of heated template. Thus, the mixed vapor must move along the chamber and the residence time of metal organic sources on the surface of substrates would be extended.

In order to research the utilization ratio of metal organic sources, the concentration of Gd(tmhd)$_3$, Y(tmhd)$_3$, Ba(tmhd)$_2$·(1,10-phenanthroline)$_2$ and Cu(tmhd)$_2$ were respectively 0.04 mol.L^{-1}, 0.04 mol.L^{-1}, 0.16 mol.L^{-1} and 0.16 mol.L^{-1}, which were kept unchanged in the precursor. The pump rate of precursor was 2.5 ml.min^{-1}. Hence, the utilization ratio of metal organic sources can be obtained through calculating the volume of deposited GdYBCO film in certain time. Meanwhile, the reel-to-reel preparation of GdYBCO films can also be researched based on the novel reaction chamber. The metal tapes pass through the slits at the two ends of the narrow channel reaction chamber and the two heating electrodes, and then are fixed on the two winding devices, which are driven by servo unit. Then, the winding speed of 0.5 m min^{-1} was adopted to prepare the 1 m-length superconducting sample.

The thickness of GdYBCO film was measured by a step profiler (Veeco Dektak 150). The texture was measured through a x-ray diffraction system (XRD, Bede D1 system) with θ-2θ scan, ω-scan, φ-scan and *Chi*-scan. Among them, the θ-2θ scan was used to characterize crystal orientation and crystal quality of GdYBCO films. The ω-scan, also known as the out-of-plane rocking curve scan, was mainly used to analyze the out-of-plane arrangement of GdYBCO grains. The φ-scan, also called the in-plane scan, was used to analyze the in-plane arrangement of GdYBCO grains. The *Chi*-scan was used to characterize the proportion of *c*-axis-oriented grains and *a*-axis-oriented grains in the prepared GdYBCO films. The surface morphology was characterized by a scanning electron microscope (SEM, JEOL7500F). The composition was characterized by an energy dispersive spectrometer (EDS, Oxford INCA). What is more, the critical current density (J_c) and critical current (I_c) at 77 K and 0 T were obtained by the Leipzig J_c–scan system [38] and four-probe-method measurement system.

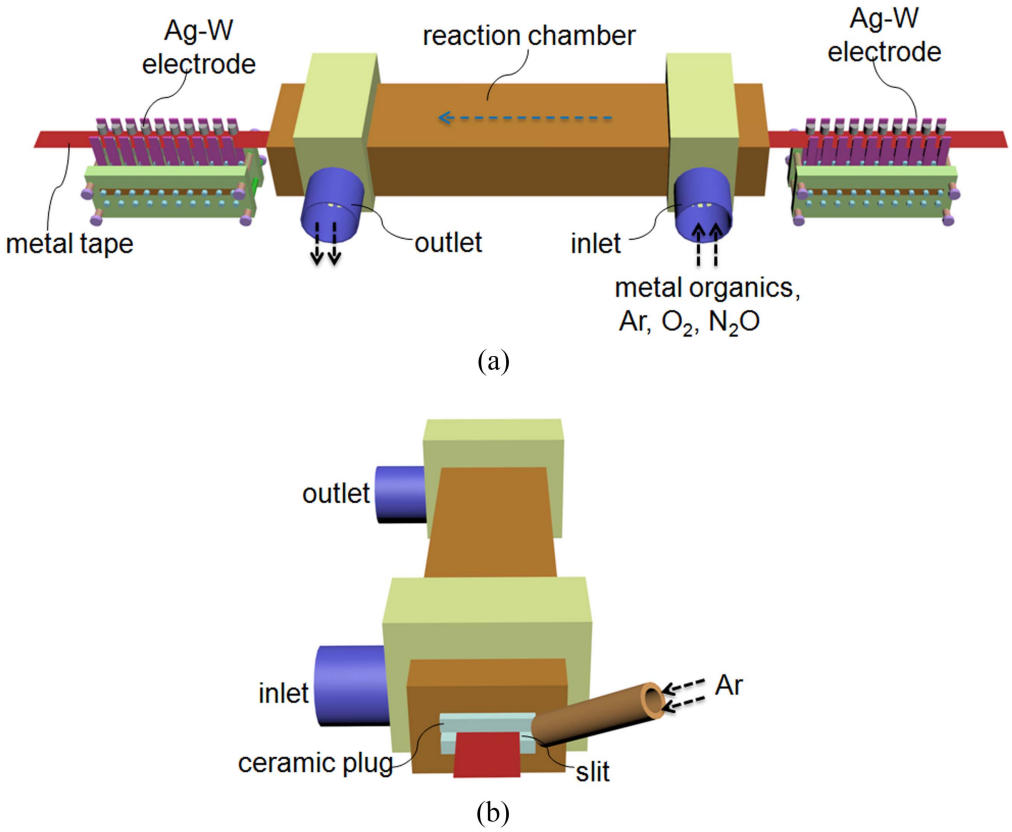

Figure 2. (a) The schematic diagram of GdYBCO film preparation based on the narrow channel reaction chamber and self-heating method; (b) the schematic diagram of the narrow channel reaction chamber.

3. Results and discussion

3.1. The utilization ratio of metal organic sources based the narrow channel chamber

There are two slits of 1 mm × 11 mm which are parallel to each other on both sides of the reaction chamber, as is shown in figure 3(a). The oxide-buffered Hastelloy metal tape was placed in the midline of the chamber through two slits. As is shown in figure 3(b), the total length of the chamber is 30 cm and the actual length of deposition zone is about 27 cm. The opening of the chamber is a rectangle of 6 mm × 12 mm and the slit is a rectangle of 1 mm × 11 mm. Figure 3(c) shows the photograph of the reaction chamber, which was made of metal copper to ensure good heat conduction.

The vapor of metal organic sources and the reaction gas were introduced into the reaction chamber. By adjusting the process condition, the double-sided GdYBCO films were prepared on the motionless double-sided buffer template and its depositing time was set for 0.5 min. Through using a step profiler, the thickness of double-sided GdYBCO films were measured and fitted, as is shown in figure 4. According to the fitting results, the average thickness ($\overline{H}$) of the double-sided GdYBCO films was approximately 1000 nm. Therefore, the actual volume (V_D) of the deposited film can be calculated, which is given by:

$$V_D = W \cdot L \cdot \overline{H}, \tag{1}$$

where $W = 10$ mm is the width of tapes and $L = 270$ mm is the length of the deposited film. Thus, the utilization ratio (R_u) of metal organic sources can be obtained by the calculation of formula:

$$R_u = \frac{6V_D}{N_A.(c_{Gd} + c_Y + c_{Ba} + c_{Cu}) \cdot v \cdot t \cdot V_{cell}}, \tag{2}$$

where $N_A \approx 6.02 \times 10^{23}$ mol^{-1} is the Avogadero constant, c_{Gd}, c_Y, c_{Ba} and c_{Cu} are the concentration of Gd(tmhd)$_3$, Y(tmhd)$_3$, Ba(tmhd)$_2$·(1,10-phenanthroline)$_2$ and Cu(tmhd)$_2$ in sequence, v is the pump rate of the precursor, and t is the depositing time. V_{cell} is the volume of unit cell, which is expressed as:

$$V_{cell} = a \cdot b \cdot c, \tag{3}$$

where a, b and c are the lattice constant. The calculated results are shown in table 1. Thus, the utilization ratio of metal organic sources, which is calculated according to the measured results of experiments, can reach 31%.

The XRD θ-2θ scan maps of one-sided GdYBCO film, which were measured at different positions along the flow direction, were shown in figure 5. The position, which was 1 cm away from the end of the inlet, was characterized by the

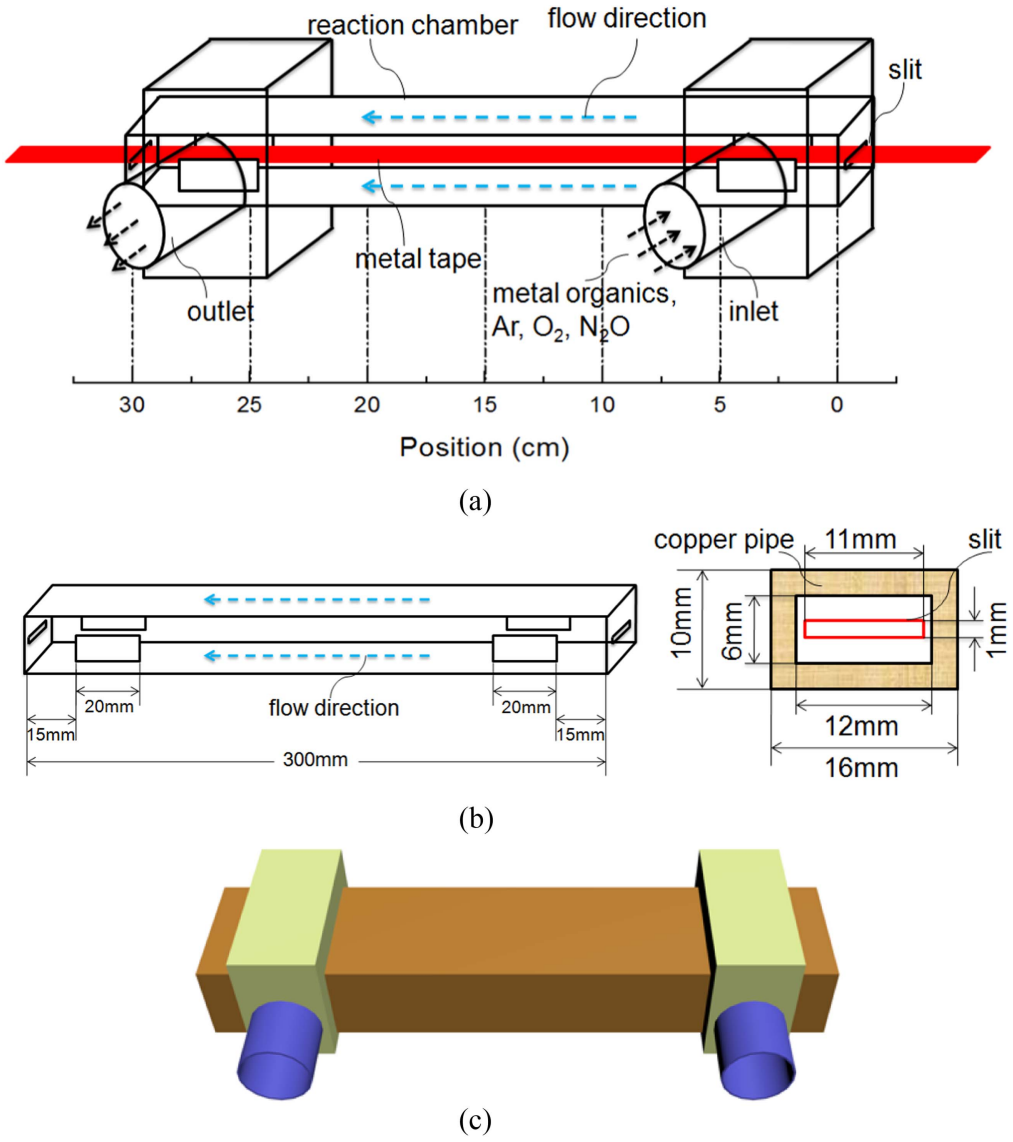

Figure 3. Schematic diagram (a), (b) and (c) of the narrow channel reaction chamber.

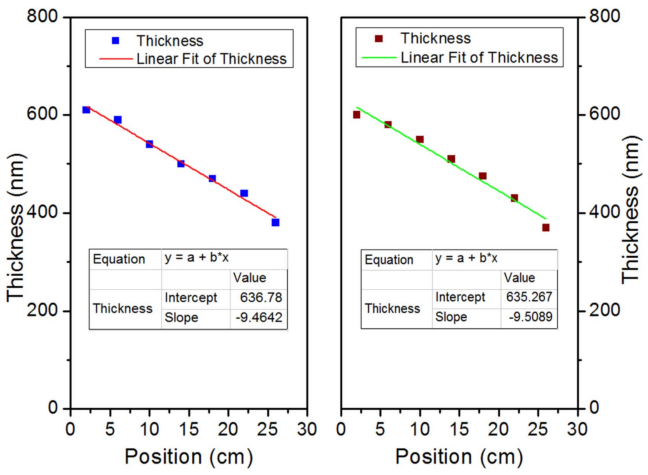

Figure 4. The transformation of thickness of double-sided GdYBCO films along the flow direction.

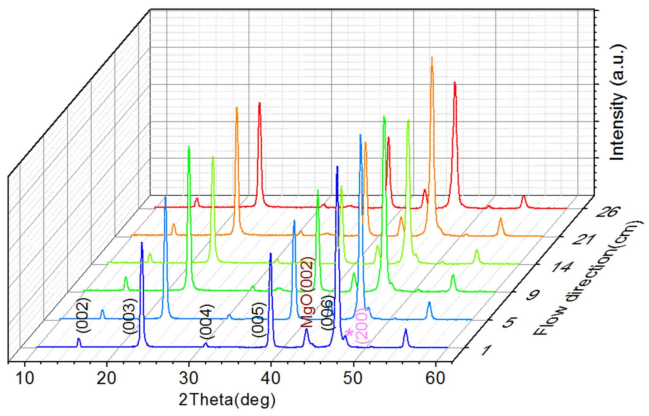

Figure 5. The XRD θ-2θ scanning patterns of one-side GdYBCO films along the flow direction.

Table 1. Consumption and utilization of metal organic sources in the experiment.

Metal organic source	Consumption in the experiment	Volume of film by complete reaction	Volume of double-sided GdYBCO film	Utilization of MO source
Dosage of MO sources Calculation	5×10^{-4} mol	8.64×10^{-9} m^3	2.7×10^{-9} m^3	31%

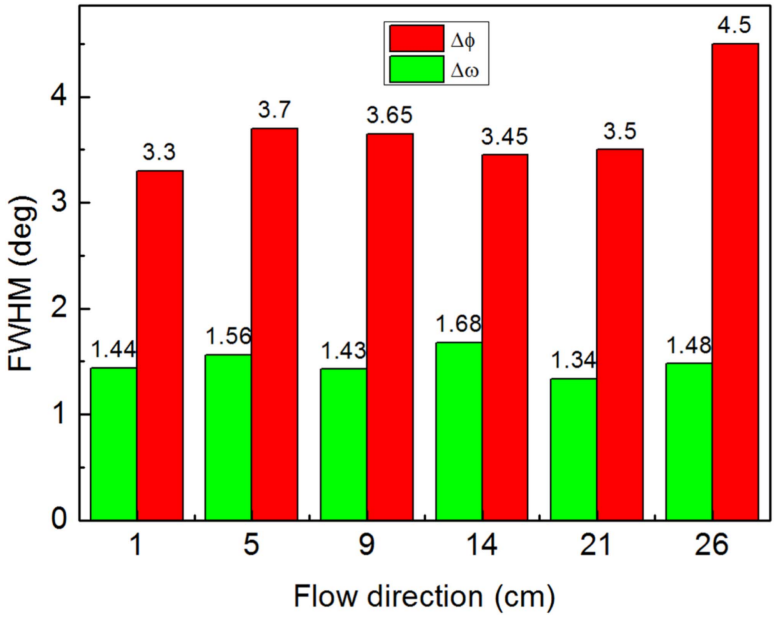

Figure 6. The transformation of FWHM values of XRD ω-scans and φ-scans along the flow direction.

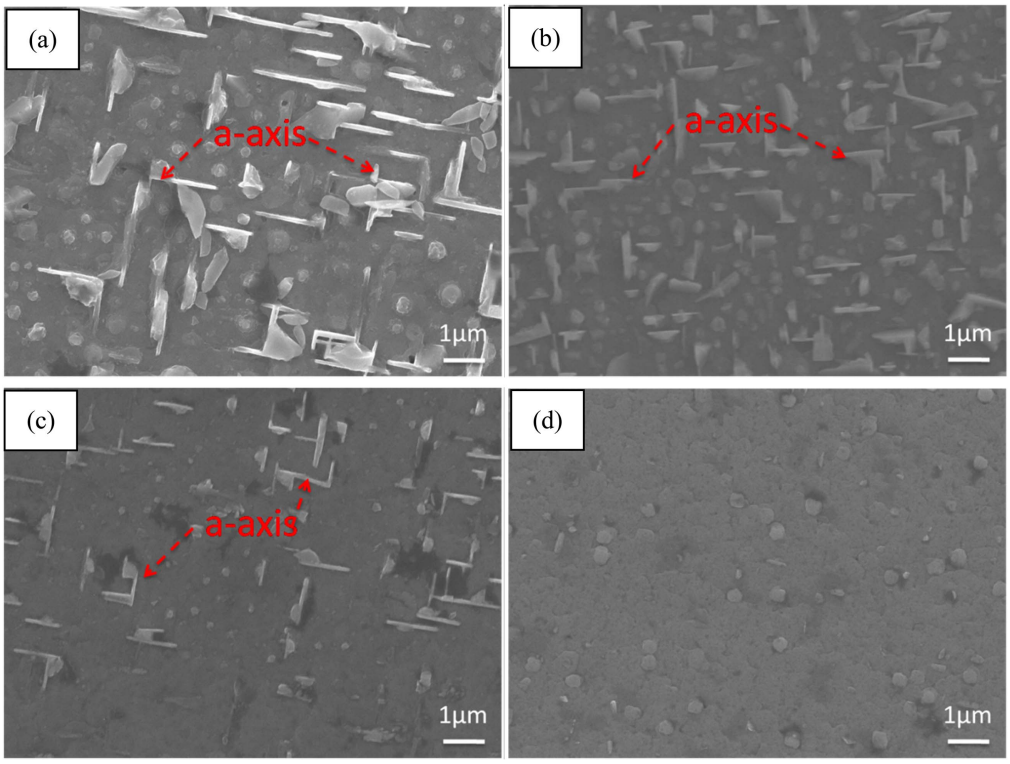

Figure 7. The SEM images of different positions of GdYBCO film from the inlet: (a) 5 cm; (b) 10 cm; (c) 15 cm; (d) 20 cm.

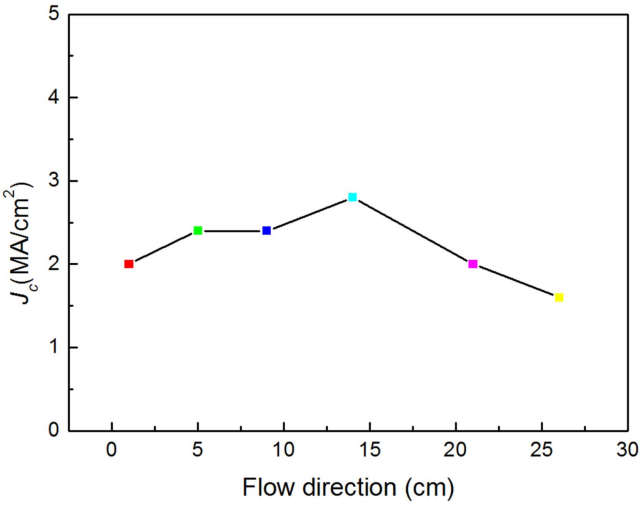

Figure 8. The transformation of J_c along the flow direction.

XRD system and there are both GdYBCO (*00l*) peaks and (*h00*) peaks in the θ-2θ curve, which indicates that there are both *c*-axis-oriented and *a*-axis-oriented GdYBCO grains in the film. This is because the surface temperature is insufficient to deposit *c*-axis-oriented grains with the increase of GdYBCO film thickness using the current heating technique. Similarly, there are GdYBCO (*00l*) peaks and (*h00*) peaks at 5 cm, 9 cm, 14 cm and 21 cm. And the intensity of (200) peak is weakened along the flow direction. However, there are only GdYBCO (*00l*) peaks other than (*h00*) peaks at the position of 26 cm, which indicates that the heating temperature is enough for the thickness of GdYBCO film here.

The XRD ω-scan of GdYBCO (005) and the XRD φ-scan of GdYBCO (103) were performed at the different positions, which were used to characterize out-of-plane and in-plane textures. Every full width at half maximum (FWHM) value by fitting every curve of the XRD ω-scan and φ-scan is listed in figure 6 at the different positions. It is obviously shown that there is not a big difference among the FWHM values of the XRD ω-scan and φ-scan except the position of the outlet.

The surface morphologies of different positions away from the inlet were characterized by a SEM, as is shown in figure 7. There are some big *a*-axis-oriented GdYBCO grains and outgrowths on the surface of position at 5 cm away from the inlet, as is shown in figure 7(a). Figures 7(b)–(d) show that the *a*-axis-oriented grains decrease and become smaller at 10 cm, 15 cm and 20 cm away from the inlet. The EDS shows that the outgrowths are CuO and Ba-Cu-O impurity phases. According to the measured results of thickness, the decrease of *a*-axis-oriented grains is due to the different deposition thickness of GdYBCO films along the flow direction, which is consistent with the measured results of XRD.

Figure 8 shows the measured value of J_c (77 K, 0 T) at different positions along the flow direction away from the inlet. Along the GdYBCO tape from 2 cm to 14 cm, the J_c values were raised from 2.0 MA.cm^{-2} to 2.8 MA.cm^{-2}. Then the J_c values declined from 2.8 MA.cm^{-2} to 1.6 MA.cm^{-2}, due to the difference of deposition rate and the variety of component.

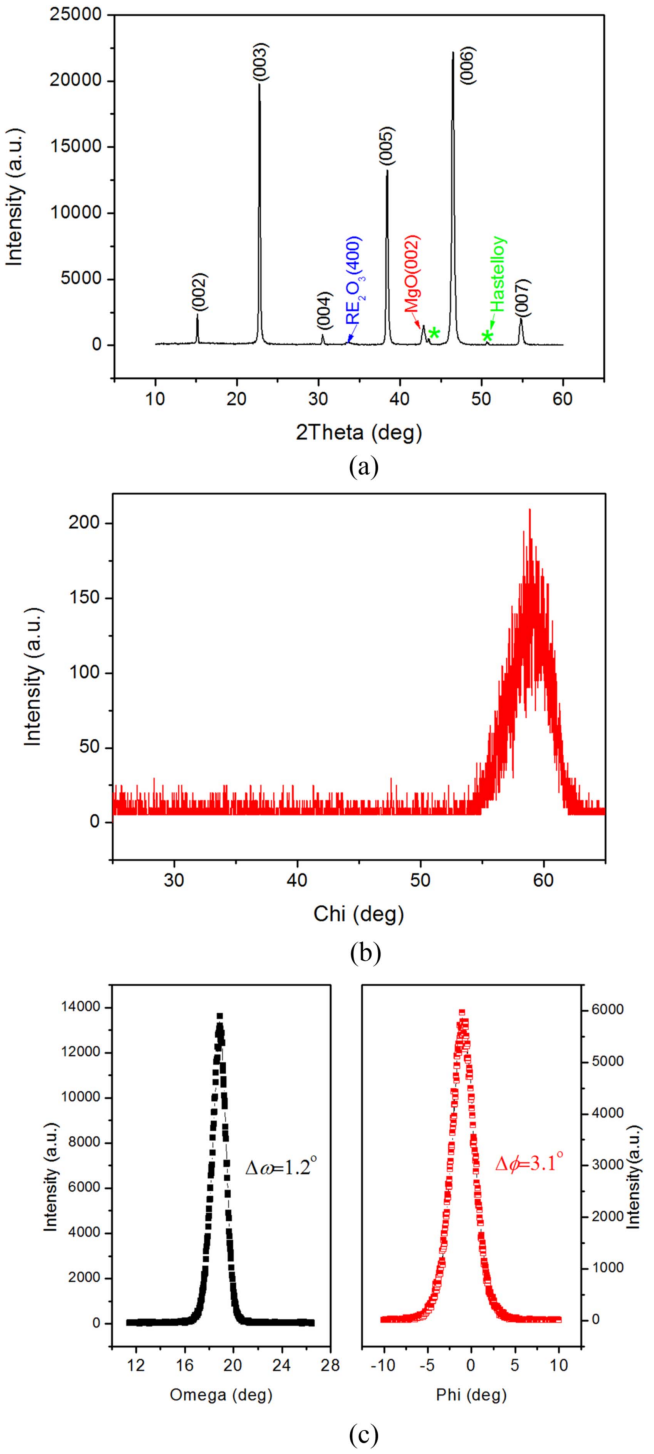

Figure 9. (a) The XRD θ-2θ scanning patterns of GdYBCO film prepared the reel-to-reel way; (b) The XRD χ-scan curves of GdYBCO (102); (b) The XRD ω-scan of GdYBCO (005) and the XRD φ-scan of GdYBCO (103).

(a)

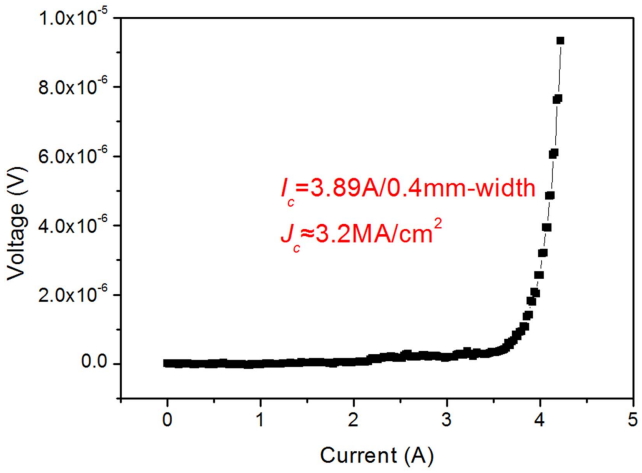

(b)

Figure 10. (a) The SEM image of GdYBCO film prepared the reel-to-reel way; (b) the measurement result of I_c of GdYBCO film.

3.2. The reel-to-reel preparation of GdYBCO films

The reel-to-reel preparation of GdYBCO films has also been prepared based on the narrow channel reaction chamber. The XRD θ-2θ scan maps of one-sided GdYBCO film, which were prepared the reel-to-reel way, was shown in figure 9(a). The GdYBCO film was characterized by the XRD system and there are only GdYBCO (*00l*) peaks without basically any other impurity diffraction peaks in the θ-2θ curve, which indicates that there are only *c*-axis-oriented grains in the film. This is because the surface temperature and the ratio of metal organic sources meet the growth of *c*-axis-oriented grains. Moreover, the XRD χ-scan of GdYBCO (102) has also been performed, which is used to characterize the *c*-axis-oriented grains and the *a*-axis-oriented grains. For the two χ-scan curves, there is only one peak around 56.6°, representing the diffraction of (102) plane of *c*-axis oriented GdYBCO grains, which indicates that all the prepared GdYBCO grains aligned their *c*-axis perpendicular to the surface of the LMO templates. The XRD ω-scan of GdYBCO (005) and the XRD φ-scan of GdYBCO (103) have also been performed; these were used to characterize out-of-plane and in-plane textures. Figure 9(c) shows the measured curves of the ω-scan and the φ-scan and the corresponding FWHM values are 1.2° and 3.1°, respectively. The results show that the biaxial texture of the prepared GdYBCO film is also very good.

The surface morphology of the superconducting film is observed via an SEM system. Figure 10(a) shows the morphology image of the prepared sample via the reel-to-reel way. The surface of GdYBCO film is very flat and the impurity precipitates did not appear. Therefore, the surface morphology is in accord with the characterization results of XRD. Meanwhile, the J_c at 77 K and 0 T are measured and can reach 3.2 MA cm^{-2}, as is shown in figure 10(b).

4. Conclusion

In this paper, we presented a narrow channel reaction chamber in order to improve the utilization ratio of metal organic sources. Results indicate that the utilization ratio of metal organic sources can reach 31%, which is basically two times as much as that of the commonly used vertical injection shower head. Thus, it indicates that the narrow channel reaction chamber is a very effective design to reduce the production cost of GdYBCO tapes based on the MOCVD process. What is more, through adjusting the process, the critical current density of 300 nm thick GdYBCO film with good biaxial texture and morphology prepared by reel-to-reel way has reached 3.2 MA cm^{-2} (77 K, 0 T), which provides a good foundation for the reel-to-reel preparation of GdYBCO films.

Acknowledgments

This work is supported by the National High-Tech R&D Program (No. 2014AA032702). Meanwhile, we also acknowledge the support of the National Natural Science Foundation of China (No. 51702265).

ORCID iDs

Ruipeng Zhao https://orcid.org/0000-0001-6994-9888

References

[1] Kosheleva N, Shahrour I, Bruzek C E, Vega G and Kolmogorov G 2016 *IEEE Trans. Appl. Supercond.* **26** 6600705
[2] Nishijima G and Kitaguchi H 2012 *IEEE Trans. Appl. Supercond.* **22** 6600304
[3] Miyoshi Y, Nishijima G, Kitaguchi H and Chaud X 2015 *J. Phys.* C **516** 31–5
[4] Mukoyama S, Yagi M, Hirano N, Amemiya N, Kashima N, Nagaya S, Izumi T and Shiohara Y 2007 *J. Phys.* C **463-465** 1150–3
[5] Masuda T *et al* 2011 *IEEE Trans. Appl. Supercond.* **21** 1030–3

[6] Jin J X, Xin Y, Wang Q L, He Y S, Cai C B, Wang Y S and Wang Z M 2014 *IEEE Trans. Appl. Supercond.* **24** 5400712
[7] Chen X Y, Jin J X, Xin Y, Shu B, Tang C L, Zhu Y P and Sun R M 2014 *IEEE Trans. Appl. Supercond.* **24** 3801606
[8] Zheng Y B, Wang Y S, Pi W, Ju P and Wang Y S 2014 *J. Phys.* C **507** 59–64
[9] Jin J X, Chen X Y, Qu R H, Fang H Y and Xin Y 2015 *J. Phys.* C **510** 48–53
[10] Gyore A, Semperger S, Farkas L and Vajda I 2005 *IEEE Trans. Appl. Supercond.* **15** 2086–9
[11] Badel A, Tixador P, Berger K and Deleglise M 2011 *Supercond. Sci. Technol.* **24** 055010
[12] Feldmann D M, Holesinger T G, Maiorov B, Zhou H, Foltyn S R, Coulter J Y and Apodoca I 2010 *Supercond. Sci. Technol.* **23** 115016
[13] Takagi Y, Takahashi Y, Nakaoka K, Yoshizumi M, Akagi N, Takahashi S, Izumi T and Shiohara Y 2012 *Phys. Proced.* **27** 200–3
[14] Kim H S, Oh S S, Ha H S, Youm D, Moon S H, Kim J H, Dou S X, Heo Y U, Wee S H and Goyal A 2014 *Sci. Rep.* **4** 04744
[15] Selvamanickam V, Gharahcheshmeh M H, Xu A, Zhang Y and Galstyan E 2015 *Supercond. Sci. Technol.* **28** 072002
[16] Leroux M, Kihlstrom K J, Holleis S, Rupich M W, Sathyamurthy S, Fleshler S, Sheng H P, Miller D J, Eley S and Kayani L 2015 *Appl. Phys. Lett.* **107** 192601
[17] Matias V, Hänisch J, Reagor D, Rowley E J and Sheehan C 2009 *IEEE Trans. Appl. Supercond.* **19** 3172–5
[18] Matias V and Hammond R H 2012 *Phys. Proced.* **36** 1440–4
[19] Muguerra H, Pescheux A C, Meledin A, Van Tendeloo G and Soubeyroux J L 2015 *J. Mater. Chem.* C **3** 11766–72
[20] Frolova A, Pompeo N, Rizzo F, Torokhtii K, Silva E, Augieri A, Celentano G, Pinto V, Armenio A A and Mancini A 2016 *IEEE Trans. Appl. Supercond.* **26** 8001205
[21] Zhang H L, Ding F Z, Gu H W, Dong Z B and Qu F 2016 *J. Alloy. Compd.* **664** 5–10
[22] Yamada H, Yamasaki H, Develos-Bagarinao K, Nakagawa Y, Mawatari Y, Nie J C, Obara H and Kosaka S 2004 *Supercond. Sci. Technol.* **17** 58–64
[23] Usoskin A, Betz U, Dietrich R and Schlenga K 2016 *IEEE Trans. Appl. Supercond.* **26** 6602304
[24] Bindi M, Botarelli A, Gauzzi A, Gianni L, Ginocchio S, Holzapfel B, Baldini A and Zannella S 2004 *Supercond. Sci. Technol.* **17** 512–6
[25] Matias V, Rowley E J, Coulter Y, Maiorov B, Holesinger T, Yung C, Glyantsev V and Moeckly B 2010 *Supercond. Sci. Technol.* **23** 014018
[26] Aytug T *et al* 2010 *Supercond. Sci. Technol.* **23** 014005
[27] Selvamanickam V, Chen Y, Shi T, Liu Y, Khatri N D, Liu J, Yao Y, Xiong X, Lei C and Soloveichik S 2013 *Supercond. Sci. Technol.* **26** 035006
[28] Zhang F, Xiong J, Zhao R P, Xue Y, Wang H, Wang Q L, He Y Y, Zhang P and Tao B W 2015 *J. Supercond. Nov. Magn.* **28** 2697–702
[29] Selvamanickam V, Gharahcheshmeh M H, Xu A, Zhang Y and Galstyan E 2015 *Supercond. Sci. Technol.* **28** 104003
[30] Selvamanickam V and Lee H G 2013 *Plasma assisted metal organic chemical vapor deposition (MOCVD)* system Patent: US8512798B2 https://www.researchgate.net/publication/302659122_Plasma_assisted_metalorganic_chemical_vapor_deposition_MOCVD_system
[31] Ko K P, Ha H S, Kim H K, Yu K K, Ko R K, Moon S H, Oh S S, Park C and Yoo S I 2007 *J. Phys.* C **463–465** 564–7
[32] Xue Y, Zhang Y H, Zhang F, Zhao R P, Wang H, Xiong J and Tao B W 2016 *J. Alloy. Compd.* **673** 47–53
[33] Ko K E, Kwon O J, Bea S H, Yoo J, Park C, Oh S S and Park Y K 2010 *Prog. Supercond. Cryogen.* **12** 17–9
[34] Sheehan C, Jung Y, Holesinger T, Feldmann D M, Edney C, Ihlefeld J F, Clem P G and Matias V 2011 *Appl. Phys. Lett.* **98** 071907
[35] Paranthaman M P, Aytug T, Stan L, Jia Q, Cantoni C and Wee S H 2014 *Supercond. Sci. Technol.* **27** 022002
[36] Zhai H Y, Christen H M, Martin P M, Zhang L and Lowndes D H 2003 *IEEE Trans. Appl. Supercond.* **13** 2622–4
[37] Zhang F, Zhao R P, Xue Y, Wang H, He Y Y, Zhang P, Tao B W, Xiong J and Li Y R 2016 *Appl. Phys.* A **122** 81
[38] Hochmuth H and Lorenz M 1996 *J. Phys.* C **265** 335–40